Quaternary International 469 (2018) 85–95

Contents lists available at ScienceDirect

Quaternary International

journal homepage: www.elsevier.com/locate/quaint

Preliminary results from Laguna Minucúa: a potentially annually resolved record of climate and environmental change for the past ~5000 years in the Mixteca Alta of Oaxaca, Mexico

Michelle Goman [a, *], Arthur Joyce [b], Steve Lund [c], Charlotte Pearson [d, 1], William Guerra [e, 2], Darren Dale [f], Douglas E. Hammond [c], Aaron J. Celestian [g]

[a] Dept. of Geography and Global Studies, Sonoma State University, Rohnert Park, CA 94928-3010, USA
[b] Dept. of Anthropology, U. of Colorado Boulder, CO 80309-0233, USA
[c] Dept. of Earth Sciences, Univ. of Southern California, Los Angeles, 90089-0740, USA
[d] Cornell Tree-Ring Laboratory Cornell University, Ithaca, NY 14853, USA
[e] Dept. of Earth and Atmospheric Sciences, Cornell University, Ithaca, NY 14853, USA
[f] Cornell High Energy Synchrotron Source, Cornell University, 277 Wilson Lab, Ithaca, NY 14853, USA
[g] Dept. of Mineral Sciences, Natural History Museum of Los Angeles County, 900 Exposition Blvd., Los Angeles, CA 90007, USA

ARTICLE INFO

Article history:
Received 20 February 2016
Received in revised form
7 November 2016
Accepted 19 January 2017
Available online 1 March 2017

Keywords:
Mesoamerica
High-resolution climate record
Precipitation
Varves
Holocene
Classic period

ABSTRACT

Despite several decades of research focusing on prehispanic human ecology, debate continues over the impact of climatic and anthropogenic landscape change on human populations in Mesoamerica. One problem in identifying the cause of this change is the lack of high-resolution paleo-environmental data from many regions. The southern Mexican highlands, in particular, have yielded few paleoenvironment data, yet have a rich and diverse cultural history.

The sedimentary record from Laguna Minucúa, located within the Sierra Madre del Sur, Oaxaca, offers an exceptional opportunity to address human and environmental interactions in the region. Minucúa is a small (~0.25 ha), currently shallow pond with no apparent inlets or outlets. We retrieved two sediment cores from the site (3.5 m and 5.6 m long). The cores are highly laminated. Core chronology was developed with paleomagnetic secular variation data and compared with couplet counts and limited radiometric measurements. These data indicate that the Minucúa record at least spans the last ~4500 ± 100 years. We discuss preliminary results that assess long-term environmental change for the region through examination of geochemical and magnetic susceptibility data. In particular, we discuss in more detail a 500 year time slice which encompasses the period known as the "Classic Collapse." The record indicates overall dry conditions but with two extended wet periods experienced between 1160 and 1120 cal yr BP and 1060–1000 cal yr BP We place our findings in the context of current archaeological and paleoclimatological research in Oaxaca.

1. Introduction

Mesoamerica, broadly defined as extending from central Mexico south to El Salvador and Honduras, has long been the focus of geographical and archaeological investigation (e.g., Holmes, 1897; Maudslay, 1889–1902; Sauer, 1941, 1957). Paleoecological research began in the 1940s and 1950s (e.g. Deevey, 1943; Sears, 1952) and has become increasingly important in understanding human impacts and land use change (e.g. Bernal et al., 2011; Deevey et al., 1979; Joyce and Goman, 2012), and more recently, climatic change and how it impacted prehispanic peoples (e.g. Bhattacharya et al., 2015; Hodell et al., 1995; Jones et al., 2015; Rodríguez-Ramírez et al., 2015). In particular, climate has been implicated as a causal factor in major periods of cultural change, especially the transition to agriculture and the Classic period collapse (e.g.

* Corresponding author.
E-mail addresses: goman@sonoma.edu (M. Goman), Arthur.Joyce@colorado.edu (A. Joyce), slund@usc.edu (S. Lund), c.pearson@ltrr.arizona.edu (C. Pearson), william.j.guerra@gmail.com (W. Guerra), darren.dale@cornell.edu (D. Dale), dhammond@usc.edu (D.E. Hammond), acelesti@usc.edu (A.J. Celestian).
[1] Present address: Laboratory of Tree Ring Research, University of Arizona, AZ 85721, USA.
[2] Present address: Chelmsford, MA Public Schools, USA.

http://dx.doi.org/10.1016/j.quaint.2017.01.027
1040-6182/

Bhattacharya et al., 2015; Haug et al., 2003; Hodell et al., 1995; Rodríguez-Ramírez et al., 2015).

Paleoclimatological studies, however, have tended to be concentrated in two regions in Mesoamerica (Fig. 1): the volcanic highlands of central Mexico (e.g. Bradbury, 1989; Conserva and Byrne, 2002; Lozano-García et al., 1993; Metcalfe and Davies, 2007; O'Hara et al., 1993) and the Maya lowlands (e.g. Brenner et al., 2002; Curtis et al., 1996, 1998; Deevey et al., 1979; Dull, 2004, 2007; Hodell et al., 2001, 1995; Jones, 1994; Leyden, 2002; Wahl et al., 2006). The geographic area between these two regions has generally poor coverage in terms of environmental and especially high-resolution climate reconstructions (Fig. 1). Research in this area has tended to focus near the coastal zone in areas below an elevation of 100 m (Goman et al., 2010, 2013, 2014; Gonzalez-Quintero and Mora-Echeverría, 1978; Jones and Voorhies, 2004; Rust and Sharer, 1988; Siemens et al., 1988; Sluyter, 1997) and to a lesser extent at higher elevations (Berrío et al., 2009; Byrne and Horn, 1989; Goman and Byrne, 1998; Lozano-García et al., 2007; Piperno et al., 2007; Piperno and Flannery, 2001). The significant lack of climate data and in particular, data of a high temporal resolution prevents a rigorous assessment of the role of climate on prehispanic cultural change in these areas. In this paper we present and discuss the climatological and environmental archives held in the sediments of Laguna Minucúa, located in the Mixteca region of Oaxaca, southern Mexico. Minucúa offers the potential for high resolution reconstructions as the sediment is composed of dark and light seasonal couplets that repeat throughout the majority of the sedimentary sequences recovered.

2. Environmental setting

The study site, Laguna Minucúa (17° 04′ 46.64N; 97° 36′ 33.30W: Fig. 1), is located in the Sierra Madre del Sur at an elevation of 2510 m. It was chosen for coring as it is one of the few extant natural lake bodies that remain in the region. The nearest weather station is located at Chalcatongo (~6 km to the southeast). Annual temperature ranges from 11 to 16 °C. Overall annual precipitation is approximately 900 mm a year; however, precipitation is highly seasonal with the rainy season running from May to October, when ~90% of all precipitation falls (Fig. 2: http://smn.cna.gob.mx).

Between elevations of 2000–2600 m the natural vegetation for the region, is dominated by various species of pine (*Pinus oaxacana, P. teocote, P leiophylla, P. lawsoni,* and *P. pringlei*) with occasional occurrences of juniper (*Juniperus* spp.), madrone (*Arbutus* spp.), and oak (*Quercus* spp.). At elevations between 2500 and 3500 m more mesophytic conditions are found, which are characterized by fir (*Abies hickelli*) in association with pine (*P. pseudostrobus*), oak, and madrone (Bersain Ortiz Jiménez, 2007). The local geology is predominantly Late Cretaceous and Tertiary arc volcanic rocks and marine forearc sediments (Moran-Zentano et al., 2007; Nieto-Samaniego et al., 2006). Soils in the area are dominated by rendzinas (Bersain Ortiz Jiménez, 2007).

Laguna Minucúa has no inlets or outlets and appears to have formed in a carbonate sink. The pond is about 0.25 ha in size. The site is surrounded on three sides by a calcareous outcrop, which has stands of *P. oaxacana* and *Quercus* spp. growing on the slope. The land slopes toward the lake from the northwest and here the vegetation has been cleared for maize agriculture. The pond surface was clear of aquatic vegetation at the time of coring and low grasses and sedges were present around the periphery. At the time of coring the water depth was ~45 cm.

3. Cultural history

The Mixteca is a mountainous region with peaks reaching 3000 m broken by a series of small highland valleys with floor elevations ranging from 1500 to 2500 m asl. The mountains descend abruptly to the Pacific Ocean in a steep escarpment, often forming a high, rugged coastline, which is interrupted in places by lowland river valleys and short stretches of coastal plain. The region was inhabited largely by Mixtec-speaking peoples in the prehispanic era as it is today. Major centers of prehispanic population and socially complex societies developed in the highland valleys, which offered the most productive agricultural land, as well as in a number of coastal lowland valleys.

Occupation in the Mixteca dates to the Paleoindian period with early sedentary villages emerging by ca. 3550 cal yr BP. (Joyce, 2010; Pérez Rodríguez, 2013). Evidence for anthropogenic erosion due to land clearance for cultivation begins as early as 3950 cal yr BP. in the highlands (Mueller et al., 2012). Between 2250 cal yr BP. and 1850 cal yr BP. perhaps a dozen urban or proto-urban hilltop centers emerged in the Mixteca at sites including Río Viejo,

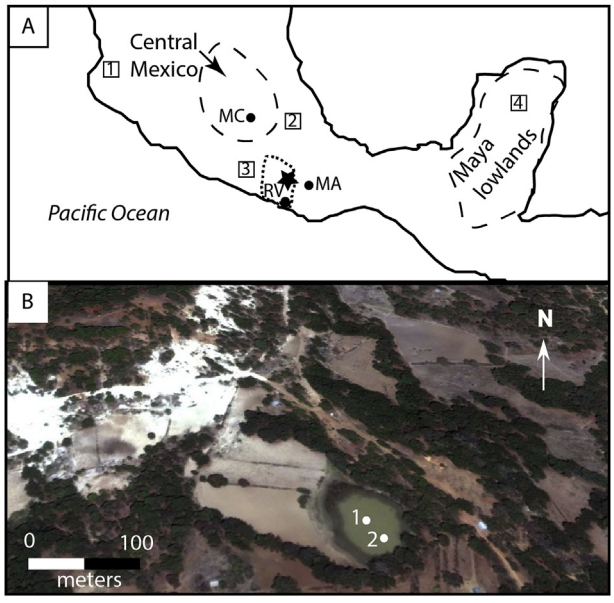

Fig. 1. A. Location of Minucúa, major archaeological sites in Oaxaca and selected high-resolution climate records. Dashed line shows Mixteca region. (Image Source: Google, Landsat). The black star indicates the location of Laguna Minucúa; RV = Río Viejo; MA = Monte Albán; MC = Mexico City; 1: Juanacatlán (Jones et al., 2015); 2: Aljojuca (Bhattacharya et al., 2015); 3: Juxtlahuaca (Lachniet et al., 2012); 4: Chichancanab (Hodell et al., 1995). B. Laguna Minucúa and its immediate vicinity. Numbers 1 and 2 show the approximate location of core locations (Image Source: Google, Digital Globe).

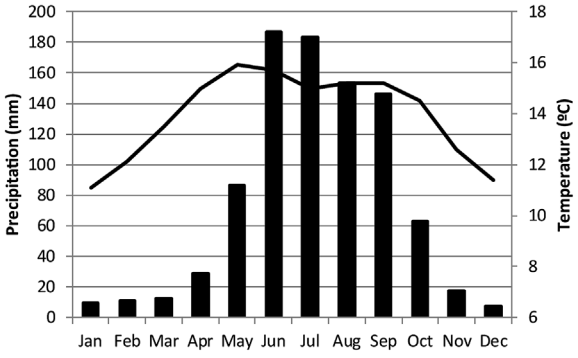

Fig. 2. Climograph for Chalcatongo (station 20178) for the period 1951–2010 (Data from Mexican Meteorological Service: http://smn.cna.gob.mx). The solid line represents temperature and the bar graph precipitation.

Huamelulpan, Yucuita, Monte Negro, Cerro Jazmín, and Cerro de las Minas (Joyce, 2010). Many of these urban centers went through a period of decline or abandonment at the end of the Formative period around 1650 cal yr BP. with several new cities developing at this time.

Unfortunately, the chronology for the Late Classic (1350–1050 cal yr BP) to the Early Postclassic (1050–750 cal yr BP) transition has not been fully worked out for much of the Mixteca, leading to questions about the culture history of this time, especially the Classic period collapse. A regional archaeological surface survey in the highlands found that populations in many areas declined by ca. 1350 cal BP. (Kowalewski et al., 2009), although evidence from excavations suggest the collapse may have occurred two or three centuries later (Joyce, 2010). On the coast where the chronology is best defined, the Classic-period state of Río Viejo collapsed at ca. 1050 cal yr BP. The Early Postclassic period seems to have been a time of political fragmentation and reduced hierarchy, although the chronological issues in the highlands mean that inferences must be tentative. By the Late Postclassic period (750–428 cal yr BP) populations had reached their prehispanic peaks in most areas and the Mixteca was dominated by numerous competing city-states. On the coast, a small-empire emerged at Tututepec. The arrival of the Spanish in the 1520s CE led to demographic collapse, resettlement, and oppression. Populations in many parts of the Mixteca have yet to return to their prehispanic levels.

4. Methods

4.1. Field work and initial analyses

In 2008 two sediment cores (MN1 and MN2) were extracted from different locations in the pond using a 5 cm diameter Livingstone corer. The cores were extruded on site into plastic tubes for transport back to the United States (Goman and Guerra, 2009). Initial observations indicated that the cores were laminated. Both cores were X-radiographed at the Cornell Veterinary School and processed for the following non-destructive parameters at the National Lacustrine Core Facility (LacCore) at the University of Minnesota using a Geotek Multi-Sensor Core Logger: gamma density, high-resolution (0.5 cm) magnetic susceptibility (HRMS) and high-resolution digital imagery. Subsequent analyses focused on the longer MN2 core.

4.2. Laboratory analyses

4.2.1. Thin sections and XRD analysis

Eight samples selected to reflect laminae from along the MN2 length were sent to the National Petrographic Service for preparation. Samples were initially dried at a low temperature; an epoxy was impregnated into each sample using a vacuum chamber. The resulting rectangle epoxied billets were oriented and mounted onto glass slides and ground to the industry standard of 30 μm thickness and a cover slip was applied. Particularly wide or clearly resolved couplets within the eight billets were selected in order to conduct microscopic characterization using a petrographic microscope. Aims were to characterize the mineralogy, interpret possible depositional process and clearly define couplet boundaries as a baseline for laminae counts and measurements.

X-ray diffraction was performed using a Proto AXRD for all diffraction analyses. This powder XRD is equipped with a copper C-ray tube, rotating sample stage, solar slits, fixed beam slits (primary slit = 1.0 mm, secondary slit = 0.5 mm, receiving slit = 0.1 mm), and an energy discriminating silicon-drift detector. Step-scans were performed at 600 W tube power from 4° – 75° 2-theta, a 0.02° step size, and 10 s/step. Oriented powders were mounted on a glass disk without ethylene glycol treatment or heating.

4.2.2. Lamination counts and measurements

These were undertaken using standard microscopic characterization and counting (Renberg, 1981) in addition to the application of *Tellervo* dendrochronological software (Brewer, 2016) on high resolution digital images obtained from LacCore. Measurement of each couplet began at the top of the dark layer and extended through to the termination of the light layer.

4.2.3. Geochemistry

The geochemistry of two separate sections of the MN2 core were examined by two different but complementary XRF analyses in order to compare course and higher resolution elemental data. These exploratory analyses permitted evaluation of laminae at differing sampling resolutions (20 μm, 200 μm, and 1 mm).

Courser grade scanning XRF analysis of MN2 core drive 3 was completed at the Inorganic Geochemistry lab of the Large Lakes Observatory (LLO) using a Cox Analytical Systems ITRAX scanner. The entire drive (230–130 cm) was scanned at 1 mm resolution and an 8 cm subsection of the drive (from 155 to 147 cm) was run at 200 μm resolution. The XRF data were collected from an 8-mm-wide strip of the core push, which was centered within a broader 2-cm-wide area about the middle of the core drive. Both runs used a dwell time of 45 s per measurement.

In order to improve on the 200 μm resolution and spatial coverage obtained by standard XRF line scans, scanning x-ray fluorescence microscopy (SXFM) was performed at the Cornell High Energy Synchrotron Source (CHESS) F3 bending-magnet beamline in an attempt to produce high resolution elemental mapping of elemental changes associated with the couplets. A single-bounce glass capillary fabricated in-house at CHESS was used to provide a 20 μm beam (incident energy of 17 KeV) with an incident flux of ~3×10^9 ph/s at the sample. A single-element Vortex silicon drift detector with DXP digital signal processor was used to detect fluorescent x-rays. The detector was mounted at 90° with respect to the incident x-ray beam to minimize Compton and Thomson scattering. The sample was mounted at 45° to the incident beam and scanned through the x-ray beam with a resolution of 100 μm × 200 μm, representing a slight improvement on the ITRAX data. X-ray spectra were analyzed using the PyMCA software package (Solé et al., 2007), with analyses calibrated using NIST Standard Reference Material 2704. Resulting SXFM element maps were made of a section of MN2 drive 9, covering the core depths of 498.5–491 cm.

4.2.4. Core chronology

Ten samples of organic material and bulk sediment from MN2 were submitted to the Keck and BETA Analytic labs for AMS radiocarbon dating. The top 7 cm of MN2 was sampled at 1 cm intervals and gamma counted to determine activities of ^{210}Pb (46 keV), ^{226}Ra (from its ^{214}Pb and ^{214}Bi progeny at 295, 352, and 609 keV), and ^{137}Cs (661 keV) at the University of Southern California. Gamma counting was undertaken on an Ortec well-type intrinsic Ge detector (100 cc active volume). Excess ^{210}Pb was calculated by subtracting the ^{226}Ra from the ^{210}Pb, after correcting for radon loss from the counting tubes, determined by measuring radon emanation from a composite of all intervals. An exponential function was fitted to the excess ^{210}Pb to estimate accumulation rate, assuming constant concentration in incoming sediment.

Paleomagnetic secular variation (PSV) was measured on both cores by sampling them contiguously with 2 × 2 × 2 cm cubes (Lund et al., 2016). Paleomagnetic measurements were made on all samples by first measuring their natural remanence (NRM) and

then step-wise demagnetizing the NRMs, followed by artificial, anhysteretic remanence (ARM) and finally an another artificial, saturation isothermal remanence (SIRM) was applied (Lund et al., 2016).

5. Results

5.1. Micro-facies analyses, stratigraphy and micromorphology

Two sediment cores were collected from different locations in the lake (Fig. 1B). The first core, MN1 retrieved 3.5 m of sediment and the second core, MN2, retrieved 5.6 m. The top ~30 cm of sediment in both cores consisted of water rich sediment. However, below this disturbed surface sediment both cores are continuously laminated along their entire length (Fig. 3A). The laminae consist of graded couplets which appear to be dominantly clastic in composition. The couplet begins with a mixture of sand size material which is darker in color and grades upwards into a more homogenous, compacted light colored material (Fig. 3B, C, D). Phase analyses using the JADE software package of the XRD data confirmed iron rich montmorillonite as the dominate mineral in the light colored couplet. A second phase was also present, but could not be identified because only two peaks with intensities lower than 2% of maximum montmorillonite were in the pattern. The boundary for the start of each couplet is sharp, but with some occasional downward movement of particulates (Fig. 3B).

The dark laminae are organic rich and consist of sand to silt-sized detrital quartz, feldspar and organic matter including rounded charcoal particulates and rare calcareous shell fragments. Particle size grades to finer components of these same materials before transitioning into a concentration of the extremely fine montmorillonite clays and with evidence of authigenic hydrous sulfate minerals (these can appear as yellow-orange patches) which make up the lighter half of the couplet (Fig. 3B, D, E). Within the dark lamina occasional variable sub-laminae are present (Fig. 3D). Localized patches of dendritic mineral growth perpendicular to the upper boundary of the couplet may indicate post depositional stagnation (Fig. 3D).

5.2. Geochemistry

The combined XRF and SXFM data were used to further characterize the couplets at different points within the sediment cores. We first examine the SXFM data, obtained from between 498.5 and 491 cm of drive 9 from MN2, as it provides an opportunity to examine the elemental signatures across the width of the core

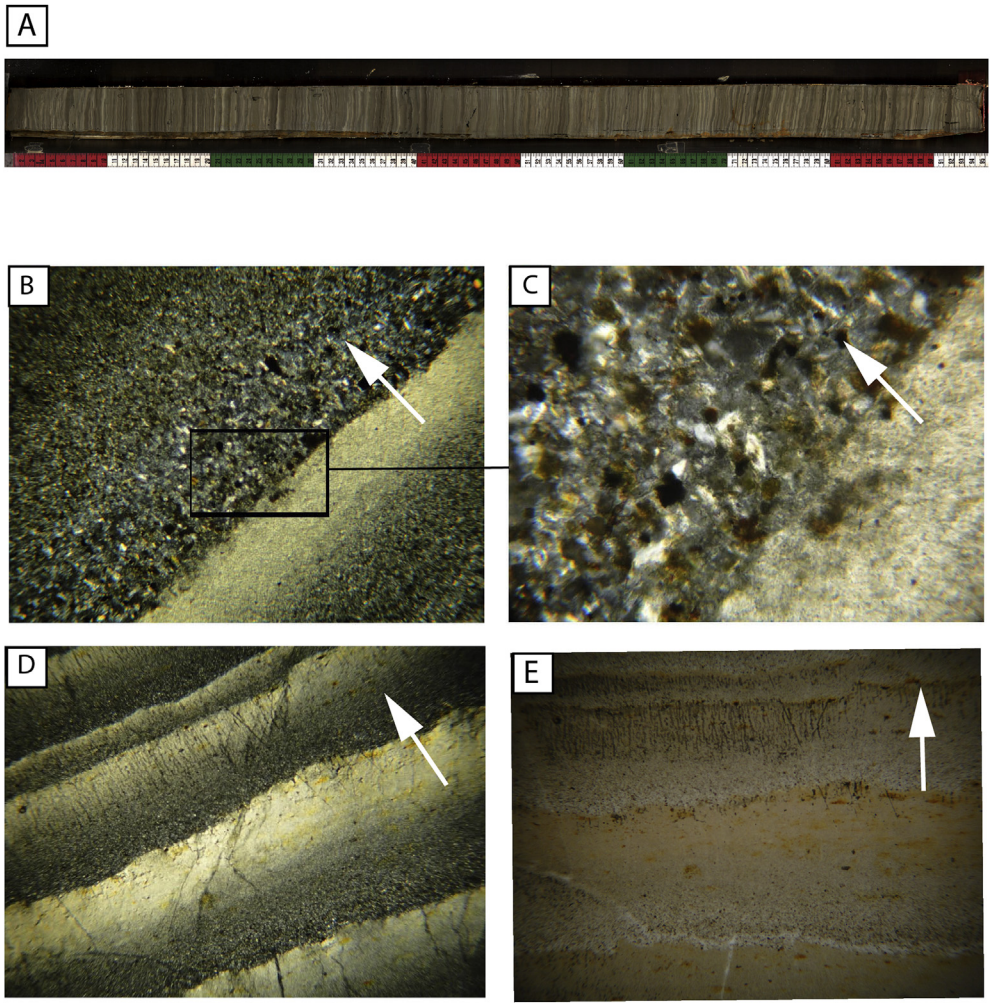

Fig. 3. A: High resolution image of MN2 230–130 cm, highlighting the nature of the light and dark couplets. 3B. Illustration of the boundary between the end of one couplet and the start of the next under crossed-polar view (x10). The boundary is sharp but with some downward movement of material. Strong grading is particularly visible in the dark phase of the couplet. 3C. Close up of boundary showing presence of quartz and feldspar grains and sand sized charcoal (x40 XPL). 3D. Illustration of micro-laminae within the dark couplets. 3E. dendritic mineral growth perpendicular to couplet layers. White arrows point towards core top.

rather than as an average of a central narrow strip. This work was experimental to see if spatially dense data could be successfully collected from un-impregnated samples. Some issues were encountered due to measures put in place to prevent desiccation of the sample during analysis and as a result elemental maps for several elements were discounted. Examples of successfully scanned elements, plus Fe and Sr maps which were still usable despite vertical artifacts and a Pb map which contained horizontal artifacts are shown in Fig. 4.

The SXFM maps showing the relative intensities (equivalent to concentrations) of each element were made of a section of core between 491 and 498.5 cm, approximately ~3670–3610 cal yr BP (Fig. 4: see section 4.2 for Chronology details). In this example the strongly laminated sequence resumes at 497 cm (after a brief period of sedimentary disturbance) with a distinct accumulation of the dark, courser grained component grading up into an unusually thick (3.5 mm) couplet compared to the others in the sequence which typically range from 0.6 to 2.2 mm wide. The darker laminae are typically shown by an increase in Ti, Fe, Cu, V, and possibly Pb relative to the light laminae and depletion of K, Ca, Rb, and Sr. The

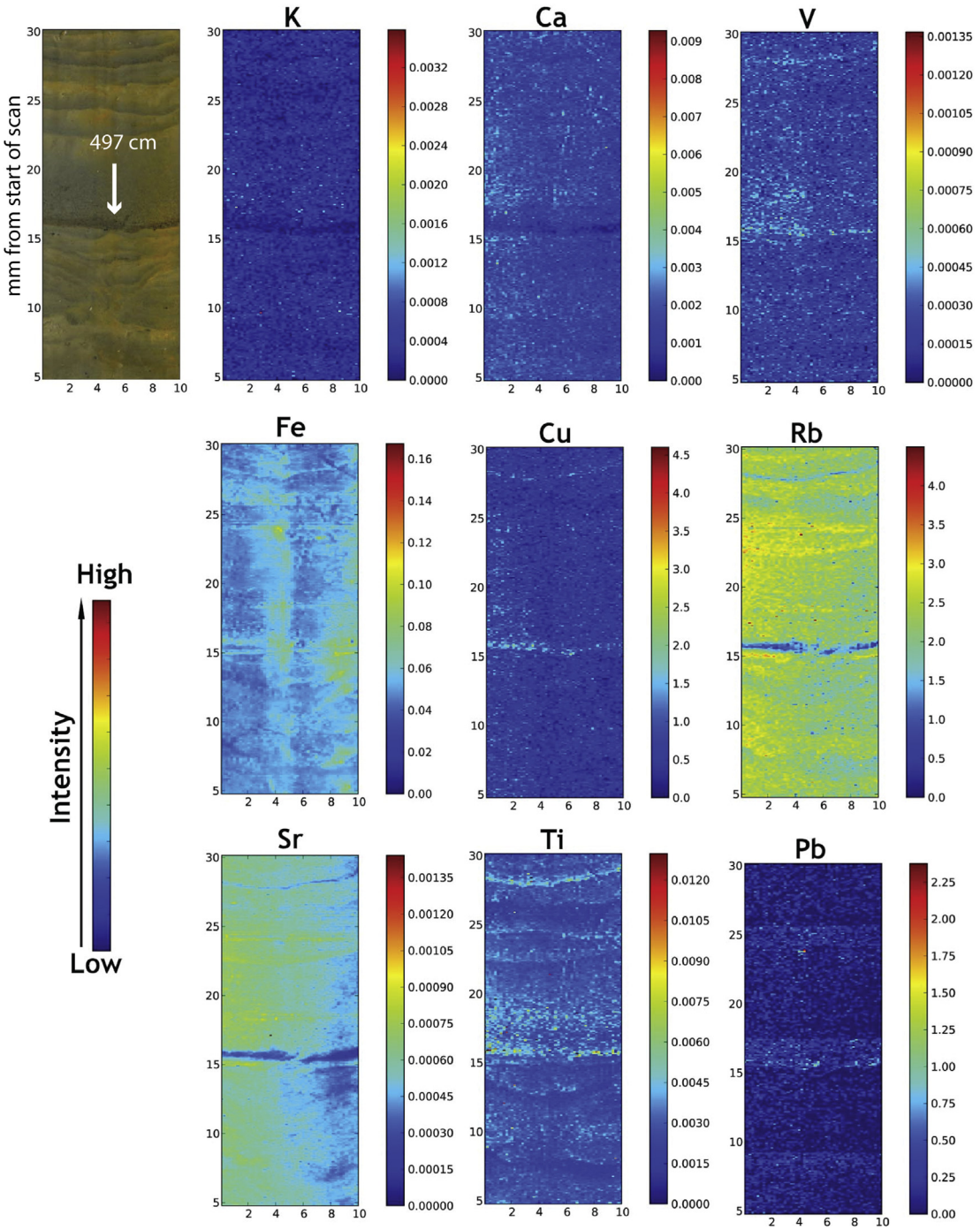

Fig. 4. The SXFM maps of 498.5–491 cm depth of MN2. Intensity values indicate relative abundances of various mapped elements. Vertical features in the Fe and Sr data are the product of condensation on the protective mylar cover used to prevent drying. The arrow marks the return to typical varve formation at 497 cm after a period of disturbance. The scan started at 498.5 cm and proceeded up drive (y-axis shows distance in millimeters from scan start).

result for Ti is particularly clear showing the graded nature of the couplet and depletion in the pale half of the couplet relative to the darker layer. This demonstrates the potential of elemental mapping to connect specific aspects of elemental change in a laminated sequence with particular clastic material and to definitively connect certain elements with clastic (biogenic or endogenic components). Further work on calibration to convert intensity data to concentrations in ppm would be beneficial in extending the utility of the technique. We would also recommend further trial analysis of impregnated and unimpregnated material.

The results from the scanning XRF data from core MN2 drive 3 (Fig. 5) complement and expand the Synchrotron findings. Elemental signatures followed two general patterns essentially mirroring the dark and light laminae. Here we highlight key elements and their signatures. The darker laminae are characterized by high Ti and Fe counts, while the lighter couplets generally show an inverse relationship. In contrast, S (not detected by the SXFM) exhibits relatively high counts in the light laminae (Fig. 5).

Regardless of the size, the couplets appear to be formed by a similar combination of conditions suggesting seasonal processes resulted in their formation (Fig. 5). Individual precipitation events are discounted as the physical process for the couplet formation. Precipitation events typically occur daily during afternoon thunderstorms in the rainy season, the rapid return of rainfall within a 24-h period or less would provide insufficient time for the lighter couplet formation. We are therefore interpreting the light and dark couplets as varves. The dark couplet representing coarser material deposited during the rainy season with included micro-laminae indicating specific precipitation events within that season, and the lighter couplet reflecting (finer-grained) clay deposition, authigenic hydrous sulfate minerals and organic reduction during the dry season (Cohen, 2003).

5.3. Chronology

Counting of the sedimentary couplets returned a count of 3922 couplets over 4.75 m of core MN2. This number of couplets is likely higher as in many instances drive tops were too disturbed to preserve couplet integrity sufficiently for accurate counts or measurements (a total of 0.85 m). If we assume an average lamina thickness of 1.21 ± 0.86 mm (3922 couplets/475 cm), then the base on core MN2 (560 cm) should be ~4600 years old.

The radiocarbon results from MN2 are presented in Table 1. One sample at 176 cm returned a radiocarbon age of 1200 ± 15 years and a near surface sample (28 cm) returned a post-bomb radiocarbon age range of 1951–1983 C.E. The remaining AMS results returned ages between 90 and 300 years, including a basal age of 300 ± 40 BP yrs (Table 1).

In order to provide an independent method of age assessment we developed a PSV chronology for both cores by comparing the PSV in the cores with other dated PSV records from North and Central America (Benson et al., 2002; Lund, 1996). The MN PSV record (utilizing MN1 and MN2) has several distinctive directional features in common with other North American sites which enables the development of a core chronology (see Lund et al., 2016). The PSV analysis indicates that the basal materials for MN2 are ~4500 ± 100 years old (Core MN1 encompasses the past ~2700 years). The basal PSV age for core MN2 (4500 years old) and varve-counting age for MN2 (~4600 years old) are not significantly different. The radiocarbon date at 176 cm from MN2 also compares well with the PSV data (Fig. 6A; Table 1).

We also have carried out ^{210}Pb and ^{137}Cs analyses on the top 7 cm of MN2, with the supported activity of ^{210}Pb determined by measuring ^{226}Ra progeny. A fit of a simple exponential function to the excess ^{210}Pb indicates an accumulation rate of 4 ± 2 mm/yr for the upper 7 cm, indicating an age of 1973–1996 CE (range of 12–35 years) at ~7 cm. The Cs data are consistent with this result, as ^{137}Cs is detectable to the bottom of the zone sampled and does not show a distinct maximum that can be interpreted as 1961–1963 CE. The post-bomb enriched radiocarbon at 28 cm also suggests that recent sedimentation has been high.

Calculated rates of sedimentation provide insight into the contrasting age data (Tables 1 and 2). The rates of sedimentation derived from the basal AMS dates are an order of magnitude higher than the other derived rates of sedimentation (Table 2). While the historic aged radiocarbon data can be wiggle matched to provide an

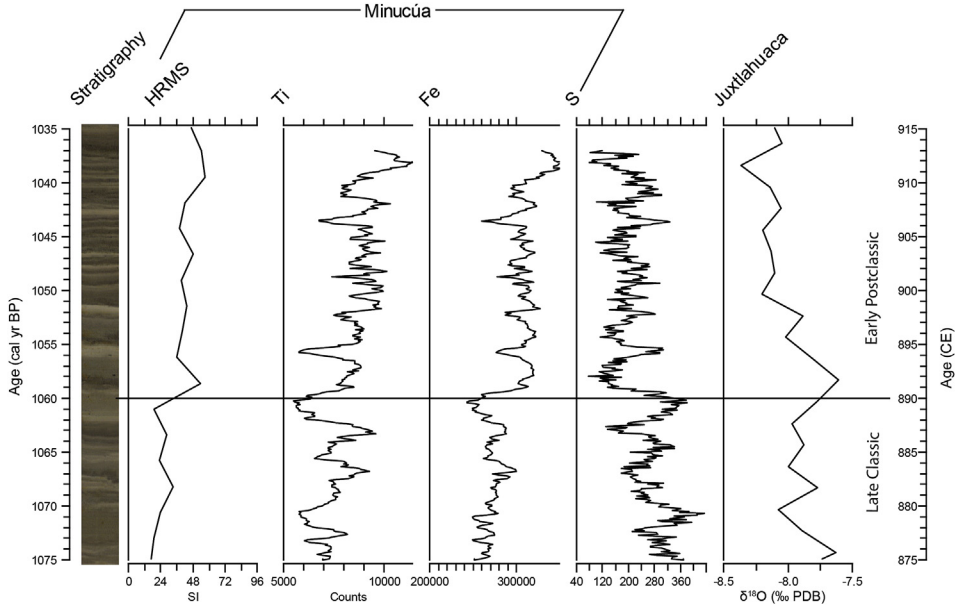

Fig. 5. High resolution image of 155–147 cm section of the MN2 core. High resolution magnetic susceptibility (HRMS) data, Ti, Fe, and S counts for the period 1075–1035 cal yr BP. Scanning XRF data was collected at 200 μm resolution and HRMS at 0.5 cm. The Juxtlahuaca δ18O speleothem record is also shown (Lachniet et al., 2012).

Table 1
AMS Radiocarbon data for MN2.

Lab	Lab #	Depth (cm)	Material	^{14}C age BP	± (1σ)	Median Age, cal yr BP (2σ)[a]
Keck	58,019	28	bulk sediment	−1710	15	−30
Keck	58,007	122	charcoal	150	15	190
Keck	58,006	147	charcoal and organic matter	150	15	190
Keck	58,020	176	bulk sediment	1200	15	1120
Keck	58,008	349	woody organics	130	15	110
Keck	58,009	399	charcoal and organic matter	125	15	110
Keck	58,005	425	charcoal	150	15	190
Keck	58,004	549	charcoal and organic matter	170	15	190
Beta	264,060	549	organic sediment	300	40	380
Beta	264,675	549	organics	90	40	110

[a] Calibrated using OxCal 4.2 (Bronk Ramsey, 2009; Hua et al., 2013; Reimer, 2013).

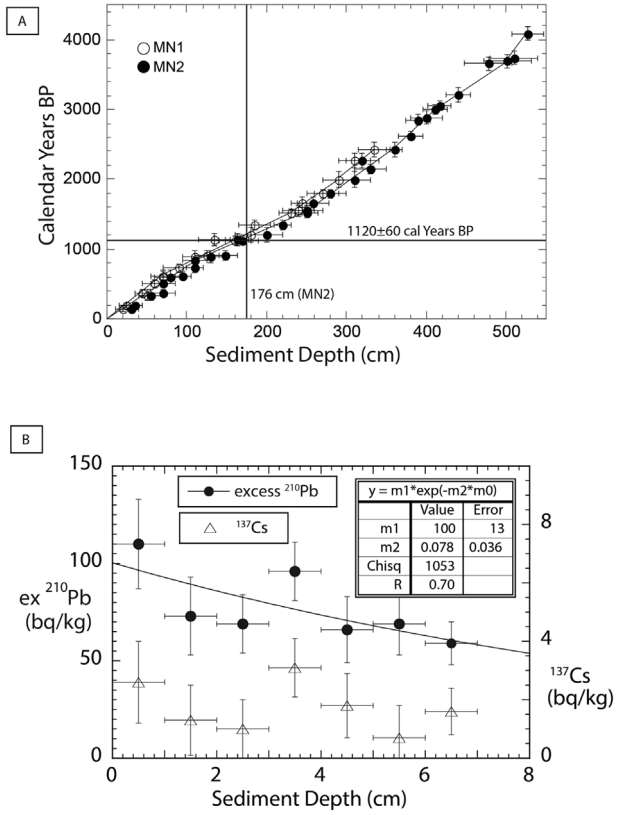

Fig. 6. A. PSV chronology for MN1 and MN2 (Lund et al., 2016). Calibrated radiocarbon age from 176 cm from MN2 is also shown. 6B. ^{210}Pb and ^{137}Cs results for the top 7 cm of MN2.

age model (S. Manning pers. comm.), the length of the core, the very high sedimentation rates derived from the historic radiocarbon ages and the intricate morphology of the couplets makes the historic radiocarbon ages and youth of the core highly unlikely. Further, investigation indicates that some of the cores were stored in a cold room that was unfortunately contaminated with radiocarbon tracers. Therefore, we exclude the historic aged radiocarbon results data from our analysis and use the PSV derived chronology.

6. Discussion

In order to show the potential of the MN sequence as a high resolution archive of climate we initially focus on the full 4500 year record derived from the magnetic susceptibility data and then focus on specific time frames in Mesoamerican cultural history, the Late Classic and earliest Early Postclassic periods. The Late Classic and Early Postclassic represent a period of political collapse throughout Oaxaca and much of Mesoamerica (Blomster, 2008; Joyce, 2010) with climate change suspected by many researchers to have been a causal factor (e.g. Bhattacharya et al., 2015; Hodell et al., 2005; Lachniet et al., 2012; Wahl et al., 2006).

It is important to note that the archaeological chronologies discussed, in particular dates associated with the "Classic Collapse", are approximate mid-points of a time-transgressive process and are based largely on radiocarbon dates. In contrast the chronology developed for Laguna Minucúa is based on varve counts, that are temporally anchored by paleomagnetic and radiocarbon data, and which allow for a much higher precision level of dating.

6.1. Long term record

In order to examine the potential climatic signal for the full sedimentary sequence we focus on the HRMS record. Both datasets indicate a range of values with a maximum 80–90 SI. The data shows centennial to decadal scale variability occurring within long-term millennial scale changes; statistical analysis (e.g. Lanci and Hirt, 2015) is however, beyond the scope of the current paper. The timeframe between 2600 and 1000 cal yr BP shows elevated magnetic susceptibility levels. Interestingly, the varve data indicates greater varve thickness variability during this time frame (1.2 ± 0.9 mm) when compared to the most recent 1000 years (1.1 ± 0.4 mm: Fig. 7) however, without the benefit of other biological or isotopic proxy data from the core, we tentatively speculate that HRMS and varves are recording millennial scale climate changes. Comparison with other climate datasets from Mesoamerica indicates that the Minucúa record may be reflecting broad regional changes associated with reorganization of the North American Monsoon (Jones et al., 2015; Metcalfe et al., 2015) and variations in the ITCZ (Haug et al., 2003).

For instance, at Lake Chichancanab, multi-proxies indicate the onset of a drier phase, with periods of intense drought, starting ~3000 years ago and ending ~1000 years ago (Hodell et al., 2005, 1995, Fig. 7). The stalagmite reconstructed precipitation record from Juxtlahuaca Cave, although not as long as the Minucúa record, indicate that wet conditions ~2400 years ago changed to drier conditions which persisted until ~1000 cal yr BP. (Lachniet et al., 2012, Fig. 7). However, without further biological proxy data our interpretation remains speculative. Prior to 2600 cal yr BP the record shows some interesting possible markers for a number of additional known global or hemispheric markers for sudden onset Holocene climatic change events (e.g. Mayewski et al., 2004). Of particular interest to the growing body of literature on global scale changes c. 4200 cal yr BP (Cullen et al., 2000; Weiss, 1997; Weiss et al., 1993; Wenxiang and Tungsheng, 2004) is the fact that a change is observable in the Minucúa record at c. 4100 BP. This certainly warrants further investigation as there is a scarcity of data

Table 2
Comparison of rates of sedimentation derived from AMS dates, PSV and couplet counts.

Method used	Calculated sedimentation rate (mm/yr)
Basal calibrated median age (Beta 264,060) of 380 cal yr BP	14.73
Basal calibrated median age (Beta 264,675) of 110 cal yr BP	49.9
PSV derived basal age of 4500 cal yr BP	1.24
Radiocarbon age at 175.9 cm (Keck 58,020) of 1120 cal yr BP	1.57
Counted couplets (N = 3922) over length of core present (475 cm)	1.21
Average couplet thickness	1.21 mm

on this event from Mesoamerica.

Varve formation ceased around 1880 CE, and magnetic susceptibility data indicate major declines towards the present (Fig. 7). Without other local proxies it is difficult to interpret these data. However, as our preliminary analysis indicates association of varve formation with the North American Monsoon and variations in the position of the ITCZ, and other proxies from across the wider region show continuation of these influences (e.g. Meko and Baisan, 2001) it seems most likely that normal sedimentation cycles may have been disrupted by human activity at this time. Evidence to support this hypothesis comes from our field survey in 2008 which identified a historic cemetery located approximately ~100 m upslope to northwest of the site. Dendrochronological analysis of twenty trees from the ridge surrounding the lake yielded ages too young for attempts to correlate with the varved sequence. Most had pith dates ~1960 CE, although one tree germinated in 1881 about the time the varves ceased to form (Guerra and Goman, unpublished). The potential to find longer lived trees such as this in the immediate vicinity of the lake may be revisited, as if a significant number of germinations could be demonstrated at this time this could be indicative of some interconnected environmental/climatic event.

6.2. Late Classic and earliest Early Postclassic periods

Here we focus on a subsection of the record from MN2 for which we have HRMS, scanning XRF and couplet measurement data (i.e. MN2 drive 3). It should be noted that the scale of data acquisition differs between the two methods, with the HRMS sampling resolution at 0.5 cm, and couplet measurements at the millimeter scale. The full drive resolution for scanning XRF was at 1 mm and a subsection at 200 μm resolution. Drive 3 encompasses ~445 years from 1400 to 955 cal yr BP. This time frame encompasses the Oaxacan archaeological periods known as the Late Classic (1330–1060 cal yr BP) and the first century of the Early Postclassic (1060–740 cal yr BP). Fig. 5 shows the data for ~40 year-time frame between 1075 and 1035 cal yr BP at 200 μm resolution. The seasonal nature of the couplets is noticeable with the darker couplets exhibiting peaks in Ti and Fe while troughs occur in the S. Closer examination of the XRF and HRMS data indicate that a statistically significant (t-test $p < 0.001$) shift in geochemistry occurs at ~1060 cal yr BP. For the period from ~1060 to 1035 cal yr BP higher magnetic susceptibility is associated with higher Ti and Fe, lower S counts and generally thinner couplets; while the preceding time (~1075–1060 cal yr BP) is associated with generally thicker couplets and low Ti, Fe, and magnetic susceptibility and higher S counts (Fig. 5).

We are interpreting the change in proxies at 1060 cal yr BP to indicate a shift from drier to wetter conditions with changes in runoff and formation of authigenic hydrous sulfate minerals

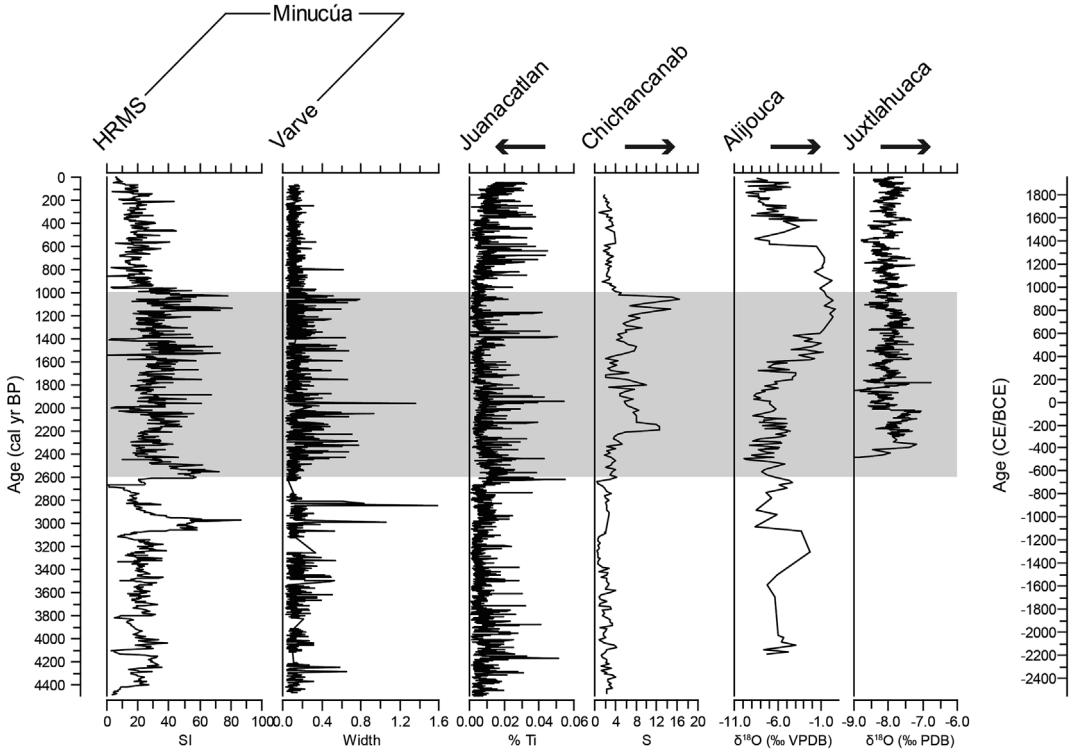

Fig. 7. HRMS and varve data for MN2 and selected high resolution climate data from Mexico. Lake records include: The titanium record from Juanacatlan (Jones et al., 2015); the sulphur record from Chichancanab (Hodell et al., 1995); oxygen isotope record from Alijouca (Bhattacharya et al., 2015); and the stalagmite oxygen isotope record from Juxtlahuaca Cave (Lachniet et al., 2012). Grey shading highlights period of higher HRMS readings at MN. Arrows indicate drier conditions.

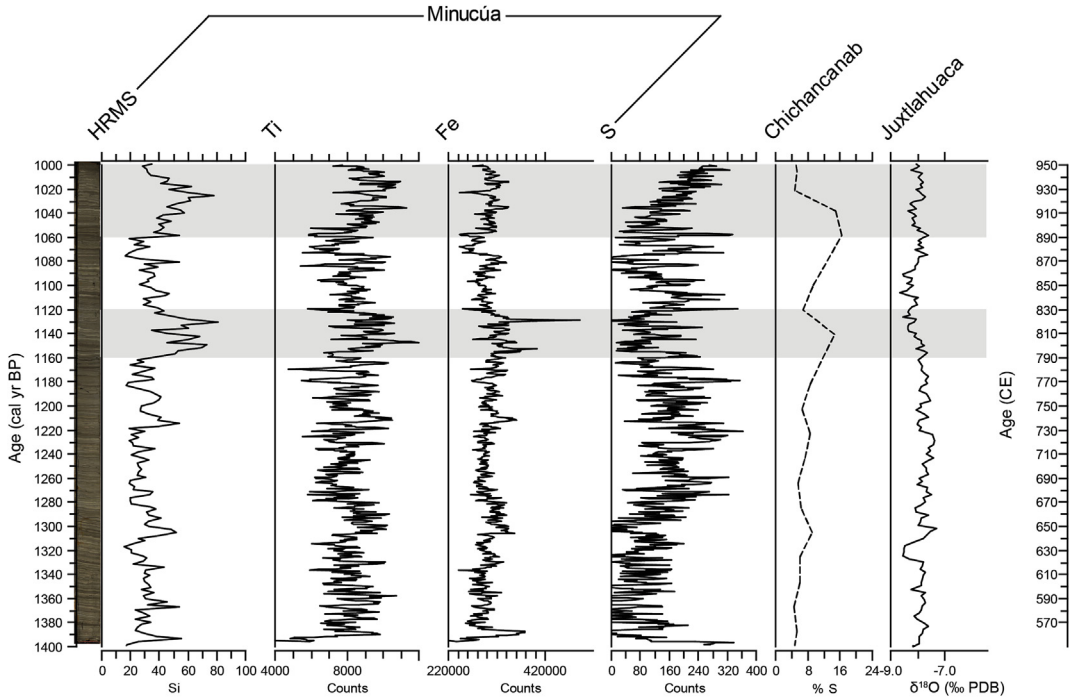

Fig. 8. High resolution image of 130–230 cm section of the MN2 core. High resolution magnetic susceptibility (HRMS) data, Ti, Fe, and S counts for the period which encompasses the Late Classic and earliest Postclassic periods. Scanning XRF data is at the 1 mm resolution, HRMS at 0.5 cm. Data are compared to selected high-resolution data sets for the same time period from Mexico; Lake Chichancanab % Sulphur (Hodell et al., 1995) and Juxtlahuaca oxygen isotope record (Lachniet et al., 2012). Shaded grey area highlights regions of inferred wetter conditions at MN.

controlling the couplet formation and width. The wider dark layer couplets that have higher magnetic susceptibility, Ti, and Fe values reflect the deposition of detrital inorganic material via surface runoff during pronounced rainy seasons while the lighter couplets represent sulfate mineral deposition during the dry season. Thick light colored couplets are reflective of pronounced dry years with extended drought permitting greater production of authigenic sulphur hydrate in Minucúa's waters. The high resolution data from Minucúa for the time frame between ~1075 and 1060 cal yr BP compares well with the Juxtlahuaca speleothem data set from Guerrero, the geographically closest high resolution data set to Minucúa (Fig. 1). At Juxtlahuaca (Fig. 5) enriched oxygen isotopic data indicates drier climate conditions between ~1075 and 1055 cal yr BP followed by depleted oxygen isotopic values indicating relatively wetter conditions (Lachniet et al., 2012). This transition from dry to wet conditions occurs at the end of the Late Classic and commences with the start of the Early Postclassic.

Examination of the high-resolution magnetic and XRF data for the 400 year time frame between 1400 and 1000 cal yr BP (Fig. 8) suggest dry conditions predominated between 1280 and 1160 cal yr BP as reflected in high S counts. This period of overall drier climate conditions, which lasted longer than a century, is comparable to the enriched $\delta^{18}O$ signal at Juxtlahuaca (Lachniet et al., 2012, Fig. 8). The period between 1160 and 1120 cal yr BP is characterized by significantly wetter conditions at Minucúa, particularly demonstrated by the high HRMS data, and peaks in Fe and Ti and declines in S counts. At Juxtlahuaca a shift to depleted $\delta^{18}O$ occurs at this time. A comparison of the MN record with existing high resolution data sets in the Yucatan indicates opposing climate conditions as the region experienced a centennial-long drought between 1180 and 1080 cal yr BP (Hodell et al., 2005). This drought has been argued to be a factor in the political collapse of the Maya (Fig. 8; Hodell et al., 2005)5a). The data from Minucúa and Juxtlahuaca (Lachniet et al., 2012) however, suggest that drought was not contemporaneous throughout Mesoamerica but rather drought was spatially and temporally transgressive (see also Yaeger and Hodell, 2008).

As in much of Mesoamerica, dramatic cultural change was experienced in the Mixteca at the end of the Classic when cities and states collapsed. In the centuries prior to this time, a number of cities including Río Viejo, Yucuñudahui, and Cerro de las Minas were the political centers of state polities (Joyce, 2010; Pérez Rodríguez, 2013; Winter, 1994). In many parts of the Mixteca and surrounding regions, such as the Valley of Oaxaca, problems with archaeological chronologies have led to debate concerning the nature and timing of the collapse (e.g. Faulseit, 2012; Kowalewski et al., 2009; Marcus and Flannery, 1990; Markens, 2008; Pérez Rodríguez et al., 2011; Winter, 2003, 1989). The clearest evidence for the Classic-Postclassic transition comes from the lower Río Verde Valley on the Pacific coast of Oaxaca where the chronology is well-developed (Hedgepeth, 2009; Joyce et al., 2001). The evidence from the lower Verde demonstrates the collapse of the Río Viejo polity ~1060 cal yr BP (Fig. 1A), settlement reorganization, and a decline in political hierarchy, but with only a modest decrease in regional population (Joyce et al., 2001).

However, we caution that although climate has been proposed as a significant causal factor in the Classic-period collapse elsewhere (e.g., Dahlin, 2002; Dunning et al., 2012; Hodell et al., 1995; Iannone, 2012; Turner and Sabloff, 2012), the collapse appears to be time transgressive throughout Mesoamerica. For instance, for the Maya, the political and in some areas demographic collapse of Classic-period polities occurred across a broad temporal time frame (~1200–900 cal yr BP; Yaeger and Hodell, 2008). While in central Mexico the collapse occurred as early as ~1300 cal yr BP at Teotihuacan (Cowgill, 2015). Given the variation in regional timing, attaching a climate driven cause is difficult to assess without high quality climate records from each region which exhibit significant differences in climate dynamics today, including the Mixteca. While

Late Classic data from Minucúa and from Juxtlahuaca (Lachniet et al., 2012) are indicating overall drier conditions at this time, We, currently defer our conclusions as to the potential impact of climate change on the Classic peoples of the Mixteca until a complete analysis of the Minucúa record and the inclusion of other proxies from the site, particularly pollen and stable isotopes are available as well as archaeological evidence for changes in agricultural practices, economics, and human health indices.

7. Conclusion

The development of a high-resolution paleoecological and paleoclimatological record at multiple timescales (annual to millennial) in the Mixteca of southern Mexico will permit the development of models of the intertwined impact of both climate and people on the landscapes of the Mixteca over the past ~5000 years. Despite its diminutive size, the sediments retrieved from Laguna Minucúa hold enormous potential to achieve this goal. While the preliminary geochemical data obtained from the cores indicates that the record is sensitive to changes in regional precipitation, detailed geochemical, isotopic and biological analysis of multiple proxies along the full core length will be required before the potential of the site is fully realized.

Acknowledgements

The research described herein was funded by the following grants: University of Colorado Innovative Grant Program (AAJ), University of Colorado Norton Fund (AAJ). We would also like to thank the Centro de Investigaciones y Estudios Superiores en Antropología Social and the people of the municipio of San Miguel el Grande. We would like to thank Raymond Mueller, Lucia Pou and Pepe Aguilar. Guerra received a LacCore Visiting Graduate Student Program scholarship to LacCore to process the cores (Funds for the LacCore Visiting Graduate Student Program are partially supported by the National Science Foundation - Instrumentation and Facilities Program as part of LacCore/CSDCO operational funding (1462297, 1338322)). Synchrotron beam work is based upon research conducted at the Cornell High Energy Synchrotron Source (CHESS) which is supported by the National Science Foundation and the National Institutes of Health/National Institute of General Medical Sciences under NSF award DMR-1332208. The contribution of Celestian was supported in part by the Natural History Museum of Los Angeles County Trelawney Endowment. We appreciate the constructive critical comments from two anonymous reviewers and from Dr. S. Starratt.

References

Benson, L., Kashgarian, M., Rye, R., Lund, S., Paillet, F., Smoot, J., Kester, C., Mensing, S., Meko, D., Lindström, S., 2002. Holocene multidecadal and multicentenial droughts affecting northern California and Nevada. Quat. Sci. Rev. 21, 659–682. http://dx.doi.org/10.1016/S0277-3791(01)00048-8.

Bernal, J.P., Lachniet, M., McCulloch, M., Mortimer, G., Morales, P., Cienfuegos, E., 2011. A speleothem record of Holocene climate variability from southwestern Mexico. Quat. Res. 75, 104–113. http://dx.doi.org/10.1016/j.yqres.2010.09.002.

Berrío, J.C., Hooghiemstra, H., Van Geel, B., Ludlow-Weichers, B., 2009. Environmental history of the dry forest biome of Guerrero, Mexico, and human impact during the last c. 2700 years. Holocene 16, 63–80. http://dx.doi.org/10.1191/0959683606hl905rp.

Bersain Ortiz Jiménez, M.C., 2007. Diagnóstico Municipal de San Miguel el Grande (Oaxaca. San Miguel El Grande).

Bhattacharya, T., Byrne, R., Böhnel, H., Wogau, K., Kienel, U., Ingram, B.L., Zimmerman, S., 2015. Cultural implications of late Holocene climate change in the Cuenca Oriental, Mexico. Proc. Natl. Acad. Sci. U. S. A. 112, 1693–1698. http://dx.doi.org/10.1073/pnas.1405653112.

Blomster, J.P., 2008. Changing cloud formations: the sociopolitics of Oaxaca in late classic and postclassic Mesoamerica. In: After Monte Alban: Transformation and Negotiation in Oaxaca, Mexico, pp. 3–46.

Bradbury, J.P., 1989. Late Quaternary lacustrine paleoenvironments in the Cuenca de México. Quat. Sci. Rev. 8, 75–100. http://dx.doi.org/10.1016/0277-3791(89)90022-X.

Brenner, M., Rosenmeier, M.F., Hodell, D.A., Curtis, J.H., 2002. Palelimnology of the Maya lowlands: long-term perspectives on interactions among climate, environment, and humans. Anc. Mesoam. 13, 141–157.

Brewer, P.W., 2016. Tellervo: a Guide for Users and Developers [WWW Document]. URL. www.tellervo.org.

Bronk Ramsey, C., 2009. Bayesian analysis of radiocarbon dates. Radiocarbon 51, 337–360.

Byrne, R., Horn, S.P., 1989. Prehistoric agriculture and forest clearance in the Sierra de los Tuxtlas, Veracruz, Mexico. Palynology 13, 181–193. http://dx.doi.org/10.1080/01916122.1989.9989360.

Cohen, A., 2003. Paleolimnology: the History and Evolution of Lake Systems. Oxford University Press, New York, NY, p. 528.

Conserva, M.E., Byrne, R., 2002. Late Holocene vegetation change in the Sierra Madre oriental of central Mexico. Quat. Res. 58, 122–129. http://dx.doi.org/10.1006/qres.2002.2348.

Cowgill, G.L., 2015. Ancient Teotihuacan: Early Urbanism in Central Mexico. Cambridge University Press, Cambridge, p. 296.

Cullen, H., Hemming, S., Hemming, G., 2000. Climate change and the collapse of the Akkadian empire: evidence from the deep sea. Geology 28, 379–382.

Curtis, J., Hodell, D., Brenner, M., 1996. Climate variability on the Yucatan Peninsula (Mexico) during the past 3500 years, and implications for Maya cultural evolution. Quat. Res. 47, 37–47. http://dx.doi.org/10.1006/qres.1996.0042.

Curtis, J.H., Brenner, M., Hodell, D., Balser, R., Islebe, G., Hooghiemstra, H., 1998. A multi-proxy study of Holocene environmental change in the Maya Lowlands of Peten, Guatemala. J. Paleolimnol. 19, 139–159. http://dx.doi.org/10.1023/A:1007968508262.

Dahlin, B.H., 2002. Climate change and the thend of the classic period in Yucatan: resolving a paradox. Anc. Mesoam. 13, 327–340. http://dx.doi.org/10.1017/S0956536102132135.

Deevey, E.S., 1943. Intento para datar las culturas medias del Vale de México mediante analisis de polen, pp. 97–105. Ciencia 4 and 5.

Deevey, E.S., Rice, D.S., Rice, P.M., Vaughan, H.H., Brenner, M., Flannery, M.S., 1979. Mayan urbanism: impact on a tropical karst environment. Sci. (New York, N.Y.) 206, 298–306. http://dx.doi.org/10.1126/science.206.4416.298.

Dull, R., 2004. An 8000-year record of vegetation, climate, and human disturbance from the Sierra de Apaneca, El Salvador. Quat. Res. 61, 159–167. http://dx.doi.org/10.1016/j.yqres.2004.01.002.

Dull, R.A., 2007. Evidence for forest clearance, agriculture, and human-induced erosion in precolumbian El Salvador. Ann. Assoc. Am. Geogr. 97, 127–141.

Dunning, N.P., Beach, T.P., Luzzadder-Beach, S., 2012. Kax and kol: collapse and resilience in lowland Maya civilization. Proc. Natl. Acad. Sci. U. S. A. 109, 3652–3657. http://dx.doi.org/10.1073/pnas.1114838109.

Faulseit, R.K., 2012. State collapse and household resilience in the Oaxaca Valley of Mexico. Lat. Am. Antiq. 23, 401–425. http://dx.doi.org/10.7183/1045-6635.23.4.401.

Goman, M., Byrne, R., 1998. A 5000-year Record of Agriculture and Tropical Forest Clearance in the Tuxtlas. The Holocene, Veracruz, Mexico. http://dx.doi.org/10.1191/095968398670396093.

Goman, M., Guerra, W., 2009. Recolección de núcleos de sedimentos y muestras para análisis paleoecológicos y muestras de núcleos de anillos de arboles para análisis dendrocronológicos. In: Joyce, A.A. (Ed.), Los Efectos Del Cambio de Clima Y Del Impacto Humano En Los Paisajes Históricos de Oaxaca. Centro de Investigaciones y Estudios Superiores en Antropología Social, Mexico City, pp. 6–15.

Goman, M., Joyce, A.A., Mueller, R.G., 2013. Paleoecological evidence for early agriculture and forest clearance in coastal Oaxaca. Polity Ecol. Form. Period Coast. Oaxaca 43–64. http://dx.doi.org/10.5876/9781607322023.c02.

Goman, M., Joyce, A., Mueller, R., Middleton, W.D., 2014. Reconstructing the formation and land use history of the Mound 2 depression at Río Viejo, Oaxaca, Mexico. Quat. Int. 342, 33–44. http://dx.doi.org/10.1016/j.quaint.2014.02.028.

Goman, M., Joyce, A., Mueller, R., Paschyn, L., 2010. Multiproxy paleoecological reconstruction of prehistoric land-use history in the western region of the lower Río Verde Valley, Oaxaca, Mexico. Holocene 20, 761–772. http://dx.doi.org/10.1177/0959683610362811.

Gonzalez-Quintero, L., Mora-Echeverría, J., 1978. Estuido arquelógicio-eclogico de un caso de explotación de recursos litorales en el Pacífico Mexicano. In: Sanchez Martínez, F. (Ed.), Arqueobotánica (Métodos Y Aplicaiones. INAH, México City, pp. 51–66.

Haug, G.H., Günther, D., Peterson, L.C., Sigman, D.M., Hughen, K.A., Aeschlimann, B., 2003. Climate and the collapse of Maya civilization. Sci. (New York, N.Y.) 299, 1731–1735. http://dx.doi.org/10.1126/science.1080444.

Hedgepeth, J., 2009. The Domestic Economy of Early Postclassic Río Viejo, Oaxaca, Mexico: Daily Practices and Worldviews of a Commoner Community. University of Colorado, Boulder.

Hodell, D.A., Brenner, M., Curtis, J.H., 2005. Terminal Classic drought in the northern Maya lowlands inferred from multiple sediment cores in Lake Chichancanab (Mexico). Quat. Sci. Rev. 24, 1413–1427. http://dx.doi.org/10.1016/j.quascirev.2004.10.013.

Hodell, D.A., Brenner, M., Curtis, J.H., Guilderson, T., 2001. Solar forcing of drought frequency in the Maya lowlands. Sci. (New York, N.Y.) 292, 1367–1370. http://dx.doi.org/10.1126/science.1057759.

Hodell, D.A., Curtis, J., Brenner, M., 1995. Possible role of climate in the collapse of classic Mayan civilization. Nature 375, 391–394. http://dx.doi.org/10.1038/

375391a0.
Holmes, W.H., 1897. Archaeological studies among the ancient cities of Mexico, Part II, monuments of chiapas, Oaxaca and the Valley of Mexico. Field Columbian Mus. Anthropol. Ser. 1, 143–338.
Hua, Q., Barbetti, M., Rakowski, A., 2013. Atmospheric radiocarbon for the period 1950–2010. Radiocarbon 55, 2059–2072.
Iannone, G., 2012. The Great Maya Droughts in Cultural Context. University Press of Colorado, Boulder, p. 448.
Jones, J.G., 1994. Pollen evidence for early settlement and agriculture in northern Belize. Palynology 18, 205–211. http://dx.doi.org/10.1080/01916122.1994.9989445.
Jones, J.G., Voorhies, B., 2004. Human and plant interactions. In: Voorhies, B. (Ed.), Coastal Collectors in the Holocene: the Chantuto People of Southwest Mexico. University Press of Florida, Gainesville, pp. 300–343.
Jones, M.D., Metcalfe, S.E., Davies, S.J., Noren, A., 2015. Late Holocene climate reorganisation and the north American monsoon. Quat. Sci. Rev. 124, 290–295.
Joyce, A., 2010. Mixtecs, Zapotecs, and Chatinos. Wiley-Blackwell, Malden, MA, p. 368.
Joyce, A.A., Goman, M., 2012. Bridging the theoretical divide in Holocene landscape studies: social and ecological approaches to ancient Oaxacan landscapes. Quat. Sci. Rev. 55, 1–22. http://dx.doi.org/10.1016/j.quascirev.2012.08.003.
Joyce, A., Bustamante, L.A., Levine, M.N., 2001. Commoner power: a case study from the classic period collapse on the Oaxaca coast. J. Archaeol. Method Theory 8, 343–385.
Kowalewski, S.A., Balkansky, A.K., Stiver Walsh, L.R., Puckhahn, T.J., Chamblee, J.F., Perez Rodriguez, V., Heredia Espinoza, V.Y., Smith, C.A., 2009. Origins of the Ñuu: Archaelology in the Mixteca Alta, Mexico. University Press of Colorado, Boulder, CO, p. 552.
Lachniet, M., Bernal, J., Asmerom, Y., 2012. A 2400 yr Mesoamerican rainfall reconstruction links climate and cultural change. Geology 40, 259–262.
Lanci, L., Hirt, A.M., 2015. Evidence of Atlantic multidecadal oscillation in the magnetic properties of Alpine lakes during the last 2500 years. Palaeogeogr. Palaeoclimatol. Palaeoecol. 440, 47–52. http://dx.doi.org/10.1016/j.palaeo.2015.08.040.
Leyden, B.W., 2002. Pollen evidence for climatic variability and cultural disturbance in the Maya Lowlands. Anc. Mesoam. 13, 85–101. http://dx.doi.org/10.1017/S0956536102131099.
Lozano-García, M.D.S., Caballero, M., Ortega, B., Rodríguez, A., Sosa, S., 2007. Tracing the effects of the little ice age in the tropical lowlands of eastern Mesoamerica. Proc. Natl. Acad. Sci. U. S. A. 104, 16200–16203. http://dx.doi.org/10.1073/pnas.0707896104.
Lozano-García, M.S., Ortega-Guerrero, B., Caballero-Miranda, M., Urrutia-Fucugauchi, J., 1993. Late pleistocene and Holocene paleoenvironments of chalco lake, Central Mexico. Quat. Res. 40, 332–342. http://dx.doi.org/10.1006/qres.1993.1086.
Lund, S., Goman, M., Joyce, A., 2016. Paleomagnetic Chronostratigraphy of Holocene Laguna Minucúa. Quaternary International, Oaxaca, Mexico (on line).
Lund, S.P., 1996. A comparison of Holocene paleomagnetic secular variation. J. Geophys. Res. 101, 8007–8024. http://dx.doi.org/10.1029/95JB00039.
Marcus, J., Flannery, K., 1990. Science and science fiction in Postclassic Oaxaca: or, "yes Virginia, there is a Monte Albán IV. In: Debating Oaxaca Archaeology. Anthropological Papers Museum of Anthropology. University of Michigan, Ann Arbor, pp. 191–205.
Markens, R., 2008. Advances in defining the Classic-Postclassic portion of the valley of Oaxaca ceramic chronology. In: Blomster, J.P. (Ed.), After Monte Alban: Transformation and Negotiation in Oaxaca, Mexico. University Press of Colorado, Boulder, pp. 49–94.
Maudslay, A.P., 1889–1902. Archaeology, Biologia Centrali Americana, 4 vols. Porter and Dulau, London.
Mayewski, P.A., Rohling, E.E., Stager, J.C., Karlén, W., Maasch, K.A., Meeker, L.D., Meyerson, E.A., Gasse, F., van Kreveld, S., Holmgren, K., Lee-Thorp, J., Rosqvist, G., Rack, F., Staubwasser, M., Schneider, R.R., Steig, E.J., 2004. Holocene climate variability. Quat. Res. 62, 243–255. http://dx.doi.org/10.1016/j.yqres.2004.07.001.
Meko, D., Baisan, C., 2001. Pilot study of latewood-width of conifers as an indicator of variability of summer rainfall in the North American monsoon region. Int. J. Climatol. 21, 697–708.
Metcalfe, S., Davies, S., 2007. Deciphering recent climate change in central Mexican lake records. Clim. Change 83, 169–186. http://dx.doi.org/10.1007/s10584-006-9152-0.
Metcalfe, S.E., Barron, J.A., Davies, S.J., 2015. The Holocene history of the North American Monsoon: "known knowns" and "known unknowns" in understanding its spatial and temporal complexity. Quat. Sci. Rev. 120, 1–27. http://dx.doi.org/10.1016/j.quascirev.2015.04.004.
Moran-Zentano, D., Cerca, M., Keppie, J., 2007. The Cenozoic tectonic and magmatic evolution of southwestern Mexico: advances and problems of interpretation. Geol. Soc. Am. Spec. Pap. 422, 71–91.
Mueller, R., Joyce, A., Borejsza, A., 2012. Alluvial archives of the Nochixtlan valley, Oaxaca, Mexico: age and significance for reconstructions of environmental change. Palaeogeogr. Palaeoclimatol. 321–322, 121–136.
Nieto-Samaniego, A.F., Alaniz-Alvarez, S.A., Silva-Romo, G., Equiza-Castro, M.H., Mendoza-Rosales, C.C., 2006. Latest Cretaceous to Miocene deformation events in the eastern Sierra Madre del Sur, Mexico, inferred from the geometry and age of major structures. Bull. Geol. Soc. Am. 118, 238–252. http://dx.doi.org/10.1130/B257330.1.
O'Hara, S.L., Street-Perrott, F.A., Burt, T.P., 1993. Accelerated soil erosion around a Mexican highland lake caused by prehispanic agriculture. Nature 362, 48–51. http://dx.doi.org/10.1038/362048a0.
Pérez Rodríguez, V., 2013. Recent advances in Mixtec archaeology. J. Archaeol. Res. 21, 75–121.
Pérez Rodríguez, V., Anderson, K.C., Neff, M.K., 2011. The Cerro Jazmín archaeological project: investigating prehispanic urbanism and its environmental impact in the Mixteca Alta, Oaxaca, Mexico. J. Field Archaeol. 36, 83–99. http://dx.doi.org/10.1179/009346911X12991472411321.
Piperno, D.R., Flannery, K.V., 2001. The earliest archaeological maize (Zea mays L.) from highland Mexico: new accelerator mass spectrometry dates and their implications. Proc. Natl. Acad. Sci. U. S. A. 98, 2101–2103. http://dx.doi.org/10.1073/pnas.98.4.2101.
Piperno, D.R., Moreno, J.E., Iriarte, J., Holst, I., Lachniet, M., Jones, J.G., Ranere, A.J., Castanzo, R., 2007. Late pleistocene and Holocene environmental history of the Iguala valley, central Balsas Watershed of Mexico. Proc. Natl. Acad. Sci. U. S. A. 104, 11874–11881. http://dx.doi.org/10.1073/pnas.0703442104.
Reimer, P., 2013. IntCal13 and Marine13 radiocarbon age calibration curves 0–50,000 Years cal BP. Radiocarbon 55, 1869–1887. http://dx.doi.org/10.2458/azu_js_rc.55.16947.
Renberg, I., 1981. Improved methods for sampling, photographing and varve-counting of varved lake sediments. Boreas 10, 255–258.
Rodríguez-Ramírez, A., Caballero, M., Roy, P., Ortega, B., Vázquez-Castro, G., Lozano-García, S., 2015. Climatic variability and human impact during the last 2000 years in western Mesoamerica: evidence of late classic (AD 600–900) and Little Ice Age drought events. Clim. Past 11, 1239–1248. http://dx.doi.org/10.5194/cp-11-1239-2015.
Rust, W.F., Sharer, R.J., 1988. Olmec settlement data from La Venta, Tabasco, Mexico. Science 242, 102–104. http://dx.doi.org/10.1126/science.242.4875.102.
Sauer, C.O., 1957. Man in the ecology of tropical America. Proc. Ninth Pac. Sci. Congr. 20, 105–110.
Sauer, C.O., 1941. The personality of Mexico. Geogr. Rev. 31, 353–364.
Sears, P.B., 1952. El análisis de pollen en la investigacion arqueologica. Tlatoani 1, 29–30.
Siemens, A.H., Hebda, R.J., Hernández, M.N., Piperno, D.R., Stein, J.K., Zolá Báez, M.G., 1988. Evidence for a cultivar and a chronology from patterned wetlands in central Veracruz, Mexico. Sci. (New York, N. Y. 242, 105–107. http://dx.doi.org/10.1126/science.242.4875.105.
Sluyter, A., 1997. Regional Holocene records of the human dimension of global change: sea-level and land-use change in prehistoric Mexico. Glob. Planet. Change 14, 127–146. http://dx.doi.org/10.1016/S0921-8181(96)00007-0.
Solé, V.A., Papillon, E., Cotte, M., Walter, P., Susini, J., 2007. A multiplatform code for the analysis of energy-dispersive X-ray fluorescence spectra. Spectrochim. Acta Part B At. Spectrosc. 62, 63–68. http://dx.doi.org/10.1016/j.sab.2006.12.002.
Turner, B.L., Sabloff, J., 2012. Classic Period collapse of the central Maya lowlands: insights about human-environment relationships for sustainability. Proc. Natl. Acad. Sci. U. S. A. 109, 13908–13914. http://dx.doi.org/10.1073/pnas.1210106109.
Wahl, D., Byrne, R., Schreiner, T., Hansen, R.D., 2006. Holocene vegetation change in the northern Petén and its implications for Maya prehistory. Quat. Res. 65, 380–389.
Weiss, H., 1997. Late Third Millennium Abrupt Climate Change and Social Collapse in West Asia and Egypt, Third Millenium BC Climate Change and Old World Collapse. Springer, Berlin Heidelberg.
Weiss, H., Courty, M., Wetterstrom, W., 1993. The genesis and collapse of third millennium north Mesopotamian civilization. Science 261, 995–1004.
Wenxiang, W., Tungsheng, L., 2004. Possible role of the Holocene event 3 on the collapse of neolithic cultures around the central plain of China. Quat. Int. 117, 153–166.
Winter, M., 2003. Monte Albán and late classic site abandonment in highland Oaxaca. In: Webb, T.I., R.W. (Eds.), The Archaeology of Settlement Abandonment in Middle America. University of Utah Press, Salt Lake City, pp. 103–119.
Winter, M., 1994. The Mixteca prior to the late postclassic. In: Nicholson, H.B., Quiñones Keber, E. (Eds.), The Mixteca-puebla Concept in Mesoamerican Archaeology. Labyrinthos, Culver City, CA, pp. 201–221.
Winter, M., 1989. From classic to post-classic in pre-hispanic Oaxaca, Mexico. In: Diehl, R.A., Berlo, J.C. (Eds.), Mesoamerica after the Decline of Teotihuacan, A.D. 700-900. Dunbarton Oaks, Washington, D.C, pp. 123–130.
Yaeger, J., Hodell, D., 2008. The Collapse of Maya Civilization: Assessing the Interaction of Culture, Climate, and Environment. El Niño, Catastrophism, and Culture Change, pp. 187–242.